THE UNIVERSITY *of* EDINBURGH

Edinburgh Research Explorer

Using the SEIR model to constrain the role of contaminated fomites in spreading an epidemic: an application to COVID-19 in the UK

OPEN ACCESS

Research article

Using the SEIR model to constrain the role of contaminated fomites in spreading an epidemic: an application to COVID-19 in the UK

Avery Meiksin

School of Physics and Astronomy
University of Edinburgh
James Clerk Maxwell Building
Peter Guthrie Tait Road
Edinburgh
EH9 3FD
meiksin@ed.ac.uk

Abstract: The use of the SEIR model of compartmentalized population dynamics with an added fomite term is analysed as a means of statistically quantifying the contribution of contaminated fomites to the spread of a viral epidemic. It is shown that for normally expected lifetimes of a virus on fomites, the dynamics of the populations are nearly indistinguishable from the case without fomites. With additional information, such as the change in social contacts following a lockdown, however, it is shown that, under the assumption that the reproduction number for direct infection is proportional to the number of social contacts, the population dynamics may be used to place meaningful statistical constraints on the role of fomites that are not affected by the lockdown. The case of the Spring 2020 UK lockdown in response to COVID-19 is presented as an illustration. An upper limit is found on the transmission rate by contaminated fomites of fewer than 1 in 30 per day per infectious person (95% CL) when social contact information is taken into account. Applied to postal deliveries and food packaging, the upper limit on the contaminated fomite transmission rate corresponds to a probability below 1 in 70 (95% CL) that a contaminated fomite transmits the infection. The method presented here may be helpful for guiding health policy over the contribution of some fomites to the spread of infection in other epidemics until more complete risk assessments based on mechanistic modelling or epidemiological investigations may be completed.

Keywords: COVID-19; epidemics; indirect transmission; infectious disease epidemiology; mathematical modelling; population dynamics; SARS-CoV-2

1. Introduction

Infectious diseases caused by viruses are communicated through several routes. These include transmission by direct contact, respiratory droplets, airborne droplet nuclei (aerosols), and indirect transmission through contaminated environmental objects (fomites). Whilst transmission through direct contact and droplets are well established for many viruses, the role of transmission by contaminated aerosols and fomites has long been uncertain [8, 18, 28, 29]. Contaminated fomites have been implicated in the transmission of some respiratory viruses (rhinovirus, respiratory syncytial virus and influenza) and gastrointestinal viruses (rotavirus, Norwalk-like viruses, hepatitis A) [6, 49, 27, 28]. Evidence has been mounting for transmission through fomites for the novel coronaviruses SARS-CoV and MERS-CoV [41, 28], and posing some concern for SARS-CoV-2 [38, 5].

The effectiveness of fomites for transmitting an infectious disease depends on several factors. The development of the infection depends on the dosage received from the fomite, quantified through the dose-response function. The viral dose delivered to a fomite is affected by the pathogenicity of the virus and the immune status of the host. The survivability of the virus on a fomite depends on several variables, including the physical properties of the fomite, the suspending medium, the initial viral titer, the virus strain and environmental variables such as the temperature, humidity and ultra-violet light irradiation level. Respiratory viruses are able to remain viable on surfaces for periods of several hours to days, depending on type and environment; viable enteric viruses may survive on a surface for more than a month [8, 48, 29].

Direct assessments of the degree to which an epidemic is spread through fomites is often frustrated by insufficient quantitative epidemiological data, while evidence obtained through cross-examination is generally circumstantial [6]. An alternative is to mathematically model the spread using known properties of the virus and the population, informed by laboratory measurements of transfer rates of viruses between fomites and humans and behavioural data regarding human interaction with fomites where possible [48]. Methods have included both mechanistic [49, 27] and stochastic approaches [45].

The COVID-19 pandemic has generated considerable effort to understanding the dominant transmission mechanisms. A respiratory illness caused by the SARS-CoV-2 virus, COVID-19 is believed to be transmitted primarily through viral-loaded respiratory droplets and aerosols and contact with an infectious person, along with a suspected contribution from contaminated fomites [53, 36, 57, 5]. As for other viral respiratory infections, establishing the transmission role of fomites and respiratory aerosols is difficult [30, 35]. Whilst viable amounts of virus survive under laboratory conditions on contaminated surfaces [51], and fomites in proximity to an infectious patient can show traces of the virus RNA [26, 38], viable viruses may not survive in a natural environment in sufficient concentration to transmit the infection. On the other hand, prolonged infectivity has been measured on organic surfaces such as skin [19] and in a protein-rich environment [42], although a standardized sanitation regimen is effective in substantially reducing the contamination of fomites in a closed environment such as a hospital room [10]. Even when fomite contamination is found, it may be in the presence of patients carrying the illness so that the direction of contamination is uncertain [53]. Indirect evidence supports the possibility of transmission through fomites. For instance, a comparison between groups with and without regular hand hygiene suggests good hand hygiene reduces the transmission [2, 31].

Current assessments suggest fomites are a minor transmission route of COVID-19 [7, 37]. It has been argued none of the evidence for transmission of infectious amounts of the SARS-CoV-2 virus

by fomites has been foolproof, and that the mere fact that wearing face coverings in China severely curtailed the spread of the disease shows that transmission by fomites is not a main driver of the epidemic [17]. No attempt was made to quantify this statement, but the principle is sound: the degree to which an infection is transmitted through air rather than by contaminated fomites will make the wearing of face coverings more effective at curtailing the spread [1]. Quantitative Microbial Risk Assessment (QMRA) using stochastic-mechanistic modelling supports the suggestion that the risk of infection from common fomites in public spaces is a minor contributor to the transmission of the SARS-CoV-2 virus compared with direct transmission, although the range of uncertainty is broad [44, 55]. Similarly, following concern over the transmission of SARS-CoV-2 through cold-chain transportation in the frozen food industry [32, 25], a stochastic QMRA analysis finds this is a low risk transmission route, but again with a large range of uncertainty [47]. On the other hand, in the closed environment of a cruise ship, mechanistic modelling suggests fomites may have accounted for as much as 30% of the infection transmission [5]. All of the QMRA stochastic-mechanistic modelling analyses of the risk of fomite transmission are limited by the still unknown dose-response function for the SARS-CoV-2 virus, as well as uncertainties in other parameters used in the models [44, 52].

In the first half of 2020, many countries instituted national lockdowns in an effort to contain the pandemic [15]. The decline in COVID-19 deaths following the lockdowns provides evidence that forms of non-pharmaceutical intervention that interrupt social contact successfully suppress the spread of the virus. The effectiveness of the lockdowns suggests direct contact between people is the main driver of the pandemic. Whilst transmission by contaminated fomites in the work place (eg through contaminated light switches, door handles, shared desks, etc.) would also be curtailed in a lockdown, contaminated fomites in homes would not be, and their contamination level would increase when a population is largely homebound because of increased usage. Additional potential fomites at risk of contamination during a lockdown include food, food packaging and post and packages generally. Indeed, public fear of contracting the illness through these fomites led to increased cleaning and even disinfection of food packages and mail [4, 30]. A sudden rise in the use of disinfectants soon after the outbreak in the US coincided with an increase in reports of poisoning, suggesting overuse of disinfectants [9]. In response, governments and health organisations advised against disinfecting food and food packaging [16], but even some of this advice was sometimes conflicting [50, 33]. In a literature review showing 63 primary studies investigating possible transmission by fomites up to June 2021, none examined possible transmission by delivered parcels or food packages available to the general public. Searching for such contaminated fomites would in fact be difficult because of their expected low numbers in general circulation [34].

Several formulations of compartmentalized models for pandemics have been developed to study the possible role of indirect transmission [3, 11, 34, 23, 56, 54]. Applications include an investigation of optimal strategies for eradicating COVID-19 in the presence of direct and indirect transmission [3]; the development of an epidemic model for the spatial spread of airborne diseases, accounting for direct transmission and indirect transmission through the diffusion of pathogens between different populations [11]; and an exploration of the general effects of including indirect transmission along with non-pharmaceutical interventions on the spread of COVID-19 [23]. Applications to COVID-19 epidemic data find a non-vanishing fomite contribution in the UK [34], China [56] and Germany and Sri Lanka [54]. It was, however, cautioned in [34] that the improvement of the fit to the UK statistics

---

[1]This conclusion presumes fomites are primarily contaminated by touch rather than by respiratory droplets or aerosols.

when contaminated fomites are included could in principle be a consequence of the fomite term's mimicking a time-dependent reproduction number for direct transmission, although this possibility was not quantified. One purpose of this paper is to address this point.

The lockdowns present a novel means of constraining the transmission rate through fomites which remain in general circulation during a lockdown, such as post and food packaging. The effectiveness of the lockdowns in curtailing the spread of the infection suggests transmission through such fomites was not a strong driver of the pandemic. A main goal of this paper is to statistically quantify this statement. The present paper expands on the previous in two regards: 1. It is shown here more generally that the contributions by direct and indirect transmission in driving an epidemic are nearly statistically indistinguishable based on data for the time-development of the populations alone in the context of a SEIR model, extended to include a contaminated fomite compartment, unless fomites remain contaminated at a level sufficient to transmit the illness for a very long time (longer than normally expected for a respiratory virus). It is shown for the UK data during lockdown, that a variation in the reproduction number over time of only a few percent is sufficient to account for a putative fomite signal. A conclusion is that a compartmentalized model alone will generally be inadequate for distinguishing a non-vanishing contribution from contaminated fomites from a small time-variation in the reproduction number. 2. When supplemented by data on the change in the number of direct social contacts once a lockdown is imposed, it is shown that the modelling of the time development of the population by an extended SEIR model can place a meaningful upper limit on the contribution of fomites to the spread of an epidemic. This approach is complementary to standard QMRA mechanistic models in that it seeks to use measured population dynamics to constrain the risk a fomite transmits an illness rather than basing the risk on detailed modelling of the transmission mechanism.

The approach is applied to the spread of COVID-19 in the UK during the lockdown in the first half of 2020. In addition to incorporating social contact data into the modelling, the analysis here differs from the earlier work [34] by using only the gradually declining death rates during the lockdown period from March to July 2020. This is done because the reported deaths during the initial onset and rapid rise of the epidemic from January until the March lockdown may have poorly reflected the actual rise as a result of uncertain or incomplete reports of deaths due to COVID-19. The exclusion of these data allows a more conservative upper limit to be placed on the role of contaminated fomites in spreading the infection.

2. Mathematical model

2.1. SEIR equations with a fomite term

The approach used is based on the standard set of SEIR differential equations, augmented by a contaminated fomite contribution [34]. The model assigns members of the population to four compartments (sub-populations): the fraction s of the initial population susceptible to infection, the fraction e exposed to an infectious individual (and became infected), the fraction i of infectious individuals, and the fraction r of removed (recovered or perished) individuals. It is assumed here that no removed individual becomes susceptible again. Sub-populations s and i are coupled through a term $R_t s i / D_i$ where R_t, the (time-dependent) reproduction number, is the average number of people an infectious person infects. The infectious period is taken to last for an average duration D_i. The duration of an exposed individual before becoming infectious is D_e.

An additional contaminated fomite compartment is added. The term f is introduced to represent the number of contaminated fomites per capita. If C_f is the average number of fomites a person comes into contact with per day, then $C_f i$ is the per capita number of fomites contaminated per day. (The possibility of cross-fomite contamination is not included.) For simplicity, a fomite that comes into close proximity to an infectious person is considered contaminated, and the average effectiveness of the contaminated fomite to transmit the infection is quantified through the transmittivity T_f, representing the average number of members of the susceptible population a contaminated fomite infects on contact. The coupling term between the susceptible population and contaminated fomites is then $T_f s f / D_f$. This represents the transmission rate per capita to an average T_f members of the susceptible population per capita by a number f of contaminated fomites per capita for the average duration D_f for which a contaminated fomite is infectious. The susceptible, exposed and infectious fractions depend only on the product $N_f = C_f T_f$. The epidemic is initiated by the introduction of exposed and infectious carriers at the respective rates c_e and c_i per capita (of the initial total population).

The model equations are

$$
\begin{aligned}
\frac{ds}{dt} &= -\left(\frac{R_t}{D_i}i + \frac{N_f}{D_f}f_*\right)s, \\
\frac{de}{dt} &= \left(\frac{R_t}{D_i}i + \frac{N_f}{D_f}f_*\right)s - \frac{e}{D_e} + c_e, \\
\frac{di}{dt} &= \frac{e}{D_e} - \frac{i}{D_i} + c_i, \\
\frac{df_*}{dt} &= i - \frac{f_*}{D_f}.
\end{aligned}
\tag{2.1}
$$

Here, the variable $f_* = f/C_f$ has been introduced to explicitly show the dependence of the infectious population on only N_f. Initially, $R_t = R_0$, where R_0 is the basic reproduction number when the epidemic starts.

In the Appendix, it is shown that the set of equations with initial conditions $s(t_0) \geq 0$, $e(t_0) \geq 0$, $i(t_0) \geq 0$ and $f_*(t_0) \geq 0$ presents a mathematically and epidemiologically well-posed model, just as for the classic SEIR equations without a contaminated fomite term [21]. The SEIR model integral constraint is modified to (assuming constant R_t, N_f and D_i),

$$
\begin{aligned}
e(t) \;+\; & i(t) + s(t) + \frac{N_f f_*(t) - \log s(t)}{R_{t,f}} \\
&= e(t_0) + i(t_0) + s(t_0) + \frac{N_f f_*(t_0) - \log s(t_0)}{R_{t,f}} + \int_{t_0}^t dt' \left[c_e(t') + c_i(t')\right],
\end{aligned}
\tag{2.2}
$$

where $R_{t,f} = R_t + N_f D_i$. A disease-free equilibrium is found for a non-vanishing susceptible fraction s_{eq}, given by the unique root of

$$
e(t_0) + i(t_0) + s(t_0) + \frac{N_f}{R_{t,f}}f_*(t_0) + \frac{1}{R_{t,f}}\log\frac{s_{eq}}{s(t_0)} - s_{eq} + \int_{t_0}^\infty dt' \left[c_e(t' + c_i(t')\right] = 0,
\tag{2.3}
$$

provided $c_e \to 0$ and $c_i \to 0$ for $t \to \infty$ (and their time integrals converge). The standard SEIR results are recovered for $N_f = c_e = c_i = 0$. The disease-free equilibrium point is found to be neutrally unstable

for $R_{t,f}s_{eq} > 1$ and neutrally stable otherwise. The analyses in [3, 11, 23, 56, 54] similarly conclude that contaminated fomites contribute additively to the reproduction number for direct transmission to determine the stability of an equilibrium point of the epidemic.

The solution to the contaminated fomite equation may be expressed in terms of the infectious population $i(t)$ as

$$f_*(t) = f_*(t_0)e^{-(t-t_0)/D_f} + e^{-(t-t_0)/D_f} \int_{t_0}^{t} dt'\, i(t')e^{(t'-t_0)/D_f}, \tag{2.4}$$

where $f_*(t_0)$ is the value of f_* at an initial time t_0. This form shows explicitly that the number of contaminated fomites arises from the cumulative contributions from the infectious population. In the limit $D_f \ll (t - t_0)$, the contaminated fomite term is directly proportional to the instantaneous infectious population fraction when $i(t)$ varies slowly over the time interval D_f, $f_*(t) \simeq D_f i(t)$. In this limit, substitution into Eqs. (2.1) shows that the contaminated fomite term acts simply to rescale the reproduction number to $R_t + N_f D_i$, so that direct and indirect transmission may not be distinguished through the time development of the populations.[2]

The daily death rate per capita depends on the susceptible population through

$$\frac{dn_d(t)}{dt} = p_d \left[\frac{R_t(t - t_{lag})}{D_i} i(t - t_{lag}) + \frac{N_f}{D_f} f_*(t - t_{lag}) \right] s(t - t_{lag}), \tag{2.5}$$

where $n_d(t)$ is the total number of deaths per capita allowing for a lag time t_{lag} from exposure to death and p_d is the fraction of infected individuals who die.

Estimates for values of the SEIR parameters are taken from Davies et al. [12] for COVID-19 in the UK. The initial reproduction number without intervention is estimated at $R_0 = 2.68 \pm 0.57$. The average time from exposed to infectious state is taken to be $D_e = 4$ days, and the characteristic time during which an individual is infectious is taken to be $D_i = 5$ days [12]. A mean infected fatality fraction $p_d = 0.0050$ is adopted [34, 43]. Estimates for the mean lag time from onset of the infection to death range from 19 to 22 days [12, 15]. A time of 3 weeks is adopted here.

This paper concentrates on the lockdown period. Although R_t will not have changed to a new fixed value instantaneously after lockdown, for simplicity lockdown conditions are modelled by taking $R_t = R_0$ before the lockdown and $R_{t,ld}$ after. Estimates in the literature for both reproduction numbers generally do not distinguish direct transference of the virus from indirect transference through contaminated fomites.

The contribution of contaminated fomites may in principle be identified through its effect on the time dependence of the populations for finite durations of fomite contamination ($D_f > 0$). Laboratory estimates for the lifetime of viable SARS-CoV-2 viruses on various substances range from under an hour on copper to several hours on plastic [51]. When embedded in protein-rich material designed to reproduce natural concentrations, the infectivity of the virus is prolonged to as long as 4 days and possibly longer [42]. The virus was similarly found to last at least 4 days on skin at room temperature, although its survival is severely shortened in a hot environment [19]. Four representative duration times are considered here, 0.21 d and 0.41 d, typical of cardboard (95% confidence interval (CI) 0.14–0.30 d)

---

[2]The fomite contribution will alter the time dependence for long fomite contamination durations D_f compared with D_i. This may be seen by Taylor expanding $i(t) \simeq i(t_0) + i'(t_0)(t - t_0) + (1/2)i''(t_0)(t - t_0)^2$, giving the dominant behaviour $f_*(t) \simeq D_f i(t) - D_f^2 i'(t)$ for $t - t_0 \gg D_f$. Taking $i'(t) \sim i(t)/D_i$, the contribution from $i'(t)$ becomes non-negligible to the time-dependence of $f_*(t)$ when $D_f > D_i$. A more complete analysis is given in Sec. 2.2 below.

Parameter	Description	Value	Reference
R_0	initial reproduction number	$2.1 < R_0 < 3.2$	[12]
R_{ld}	post-lockdown reproduction number	$0 \leq R_{\mathrm{t,ld}} \leq 1$	[46]
T_f	contaminated fomite transmittivity	$0 \leq T_f \leq 0.3$	Assumed
D_e	duration of exposed period	4 days	[12]
D_i	duration of infectious period	5 days	[12]
D_f	duration of fomite infectious contamination	$0.2 \leq D_f \leq 4$ day	[51, 42]
c_0	peak source rate per capita	$10^{-6}\,\mathrm{day}^{-1}$	[14]
t_{c0}	time of source peak	day 77	[14]
FWHM	source distribution full width at half maximum	8 days	[14]
$\bar{f}_{\mathrm{ld}}$	mean reduction factor f_{ld} in social contacts	0.26	[24]
$\sigma_{f_{\mathrm{ld}}}$	standard deviation in f_{ld}	0.086	[24]

Table 1. Model parameters.

and plastic (95% CI 0.34–0.49 d), respectively [51], 1 d and 4 d. A summary of the assumed model parameters is provided in Table 1.

An alternative means of constraining the contaminated fomite contribution is through an independent measurement of the change in the number of social contacts, assuming the reproduction number scales in proportion to the number of social contacts. Whilst a fomite contamination rate that scales in direct proportion to the number of social contacts cannot be constrained through this means, a contaminated fomite rate that is independent of, or only weakly dependent on, the mean number of social contacts may be. Examples of such fomites include postal deliveries and food purchases. To the degree such fomites contributed to the transmission, the lockdown would have been less effective in curbing the epidemic. For instance, if matching the model to the trend in recorded deaths requires the rescaled reproduction number $(R_t + N_f D_i)$ to change by a factor smaller than the reduction in the number of social contacts, then a non-vanishing contaminated fomite contribution $(N_f \neq 0)$ may be inferred.

A prior probability distribution for the change in R_t before and after the lockdown in the UK is based on the results of the CoMix survey of social contacts during lockdown [24]. Based on the reports of nearly 4000 contacts by UK participants, the mean number of daily social contacts returned from the survey was 2.8 (with an inter-quartile range of IQR = 1-4), a substantial reduction compared with the earlier POLYMOD survey result of 10.8 (IQR = 6-14). This reduction factor is adopted to provide a normal-distributed prior on the reduction factor in R_t during the lockdown, taking into account a possible contribution from contaminated fomites. The analysis here folds together the probability distribution in the reduction in the number of social contacts under lockdown with the predictions of the SEIR model to obtain a statistical constraint on N_f. Since N_f here is assumed to apply to a contaminated fomite component that was unchanged by the lockdown, it is held constant before and after the lockdown. If additional contaminated fomites were present, then they would have contributed even more to the overall death rate, including before the lockdown.

2.2. Power-series approximate solutions

Insight into the dynamical role played by contaminated fomites is provided by an approximate power-series solution to Eqs. (2.1). The first two equations show that the role of the contaminated fomites may be absorbed into an effective reproduction number

$$\tilde{R}_t = R_t + N_f \frac{D_i}{D_f} \frac{f_*}{i}. \tag{2.6}$$

This is a formal expression, in that the time dependence of both f_* and i depend on R_t. Evaluating $\tilde{R}_t$ at its value near lockdown, however, provides an accurate description of the time dependence of the populations afterwards. This may be demonstrated through power-series solutions to Eqs. (2.1). When the removed fraction r is small, it is convenient to use r as the independent variable rather than t. Power-series solutions around $r = r_0 = r(t_0)$ after a time t_0 are sought in the form:

$$s(r) = s_0 + \sum_{n=1}^{\infty} s_n (r - r_0)^n, \qquad e(r) = e_0 + \sum_{n=1}^{\infty} e_n (r - r_0)^n, \qquad i(r) = i_0 + \sum_{n=1}^{\infty} i_n (r - r_0)^n. \tag{2.7}$$

The solution to second order is described in the Appendix. The first order coefficients are

$$s_1 = -\tilde{R}_{t0} s_0, \qquad e_1 = \tilde{R}_{t0} - \frac{D_i}{D_e} \frac{e_0}{i_0}, \qquad i_1 = \frac{D_i}{D_e} \frac{e_0}{i_0} - 1, \tag{2.8}$$

where the effective reproduction number $\tilde{R}_{t0} = R_t + (D_i/D_f)N_f f_*(r_0)/i_0$ has been defined. The role of the contaminated fomites, other than in rescaling R_t, arises only at second order (and not until even higher order for i), so that the presence of contaminated fomites may not be inferred from the time dependence of the populations unless the contaminated fomite contribution is large and with a long duration compared with the infectious state so that the higher order terms become significant.

The time development of the death rate, Eq. (2.5), is affected by contaminated fomites only at the second and higher order contributions from contaminated fomites. The role of contaminated fomites may then in principle be detected either through their second order contributions, or from independent knowledge about the reproduction number R_t. Each of these possibilities is considered in turn.

2.3. Parameter estimates for COVID-19

As a case study, Eq. (2.5) is used to model the mortality rates from COVID-19 in the UK, seeking maximum likelihood estimates for R_t and N_f. Following Flaxman et al. [15], the number of deaths is drawn from a negative binomial distribution with mean N_d and variance $N_d + N_d^2/\psi$, where N_d is the model prediction for the mean number of weekly deaths and ψ is a free parameter. In the limit $\psi \to \infty$, the distribution becomes Poisson. Following Flaxman et al. [15], ψ is drawn from a half normal distribution with mode 0 and variance 5. The two-parameter likelihood for a given model is then given by

$$\mathcal{L}(R_t, N_f) = \langle \Pi_{i=1}^{N_w} \text{Neg-bin}(w_i | N_{d,i}, N_{d,i} + N_{d,i}^2/\psi)) \rangle_\psi, \tag{2.9}$$

where the product is over the N_w weeks of the period considered, with w_i deaths in week i, having an expectation value of $N_{d,i}$ in the model, dependent on R_t and N_f, and the average $\langle \dots \rangle_\psi$ is over the half normal distribution for ψ. In order to adequately sample the likelihood, a uniformly spaced grid of width $\Delta R_t = 0.0001$ and $\Delta T_f = 0.001$ is used to cover the parameter range, corresponding to approximately 3×10^6 separate models. The averaging over ψ is carried out by gaussian quadrature. To allow for a prior distribution for the reproduction number after lockdown informed by the CoMix study, a Bayesian approach is adopted by multiplying the likelihood by the prior probability distribution for the reproduction number in lockdown as informed by the CoMix study, as described in Sec. 3.2 below.

The model parameters are fit using the post-lockdown data and before lockdown is eased. The general decline in mortality rate is well-modelled using a constant reproduction rate [15]. To seek a contribution from contaminated fomites, a two-step procedure is followed. First maximum likelihood values for R_0 and $R_{t,ld}$ are found assuming no fomites contribute ($N_f = 0$); then, for the value of R_0 obtained, the joint likelihood for $R_{t,ld}$ and $N_f (\geq 0)$ is computed to determine whether adding a contaminated fomite term increases the likelihood. This procedure is followed because R_0 is made uncertain by limitations in assessing the death rate during the rapid rise of the infections. This uncertainty could produce possibly spurious higher likelihoods into lockdown when a contaminated fomite term is added if pre-lockdown deaths are included in the likelihood. The limits obtained are conservative in that the procedure minimizes the contaminated fomite signal arising from terms that may not be absorbed into a re-scaling of $R_{t,ld}$. Since any signal found may in principle be attributable to a variation in $R_{t,ld}$ during lockdown, the signal is regarded as an upper limit to the contribution from contaminated fomites.

D_f	N_f (95% CL)	$R_{\text{t,ld}}$ (M-L)	$R_{\text{t,ld}}$ (95% CL)	N_f (M-L)
d	d^{-1}			d^{-1}
0.21	0.14	0.04	0.72	0.013
0.41	0.14	0.04	0.72	0.013
1	0.14	0.04	0.72	0.013
4	0.13	0.05	0.73	0.009

Table 2. Model results for uniform priors in N_f and $R_{\text{t,ld}}$. The columns are: (1) fomite contamination duration (days); (2) 95% confidence upper limit on N_f (per infectious person per day) and (3) the corresponding maximum likelihood value for $R_{\text{t,ld}}$; (4) 95% confidence upper limit on $R_{\text{t,ld}}$ and (5) the corresponding maximum likelihood value for N_f (per infectious person per day).

2.4. Reported mortality rates from COVID-19

The COVID-19 mortality rates compiled by the European Centre for Disease Control [3] (ECDC) are used for fitting the model parameters. The ECDC compiles data from up to 500 sources in each country each week from national and regional competent authorities.

3. Results for COVID-19 in the UK

3.1. Uniform priors

A maximum likelihood fit to the death rates from the start of lockdown in the UK on 23 March 2020 until its easing in July 2020 gives a basic reproduction number $R_0 \simeq 3.107$ and $R_{\text{t,ld}} = 0.760$ during the lockdown period, consistent with other estimates [15]. (Although not used in this analysis, after the lockdown is eased the maximum-likelihood model for the death rates until the end of August corresponds to $R_{\text{t,lde}} = 0.867$.) The solutions with contaminated fomites show only small departures in the death rates from a model with constant reproduction rate after lockdown, in accordance with the power-series approximation (see Appendix). The magnitude of the departure depends only weakly on the duration D_f of the fomite contamination for the range considered.

The joint likelihood function for $R_{\text{t,ld}}$ and N_f during lockdown is very flat, with the highest values corresponding to a ridge at $R_{\text{t,ld}} + D_i N_f \approx 0.76$ for $0.21 \leq D_f \leq 4$ d. A posterior probability distribution for $R_{\text{t,ld}}$, marginalised over N_f, is computed by summing the likelihoods for fixed $R_{\text{t,ld}}$ over all N_f contributions, followed by an overall unit normalisation over $R_{\text{t,ld}}$. The resulting posterior probability distribution for $R_{\text{t,ld}}$ is shown in the upper panel of Fig. 1 for $D_f = 0.41$. The results are nearly independent of D_f for $0.21 \leq D_f \leq 4$ d. The marginalised 95% confidence upper limits on N_f are provided in Table 2. The maximum likelihood values for $R_{\text{t,ld}}$ corresponding to the 95% confidence upper limit values for N_f are in the next column. Also shown are the marginalised 95% confidence upper limits
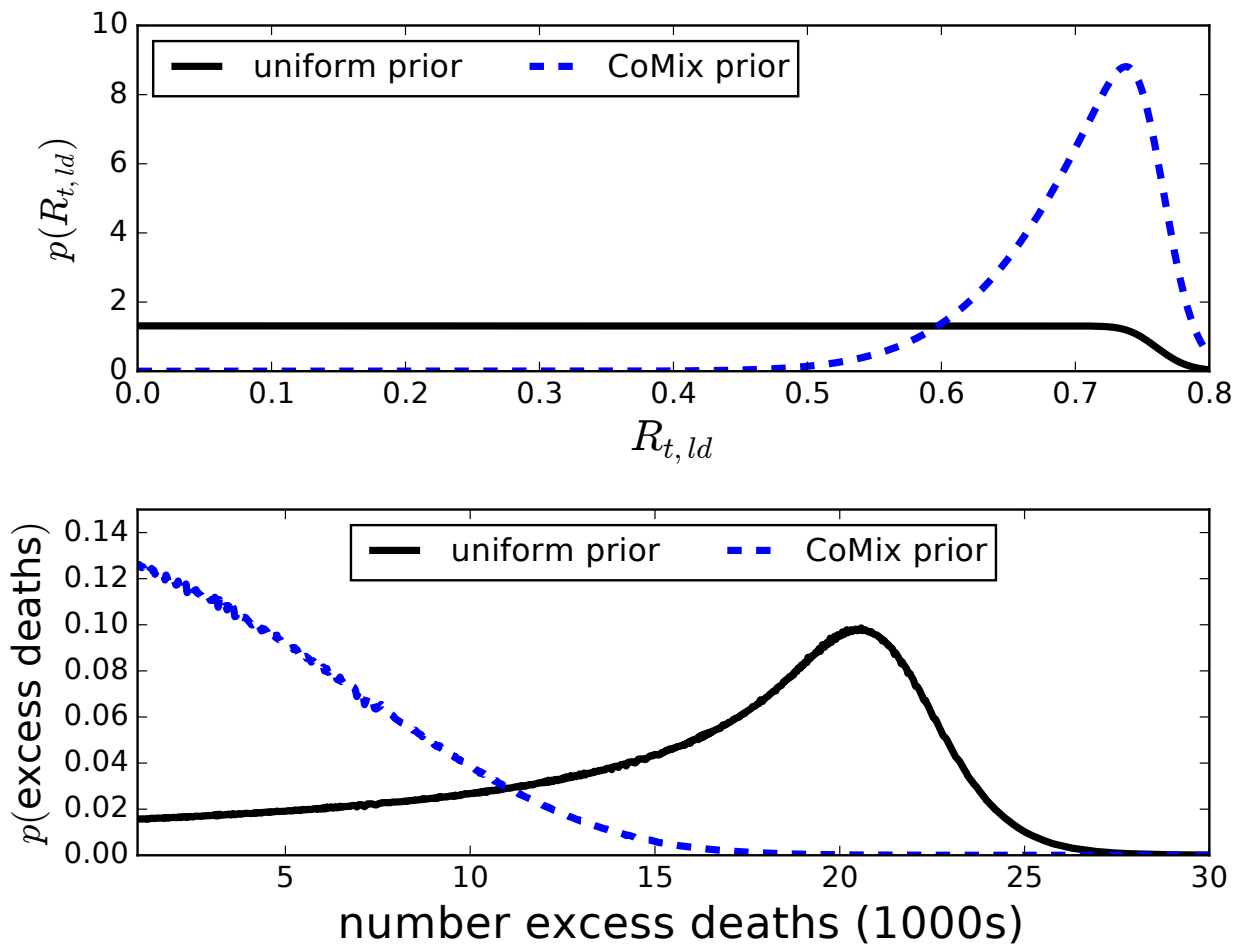
---

[3]https://www.ecdc.europa.eu/en/covid-19/data-collection

Figure 1. *Upper panel:* Marginal posterior probability density for $R_{\text{t,ld}}$, marginalised over N_f, both for a uniform prior for $R_{\text{t,ld}}$ (solid black line) and a prior based on the CoMix study (dashed blue line). *Lower panel:* Probability density for excess number of deaths from contaminated fomites over the lockdown period, both for uniform and the CoMix prior on $R_{\text{t,ld}}$. Both panels shown for $D_f = 0.41$ d; results are not very sensitive to D_f over the range considered.
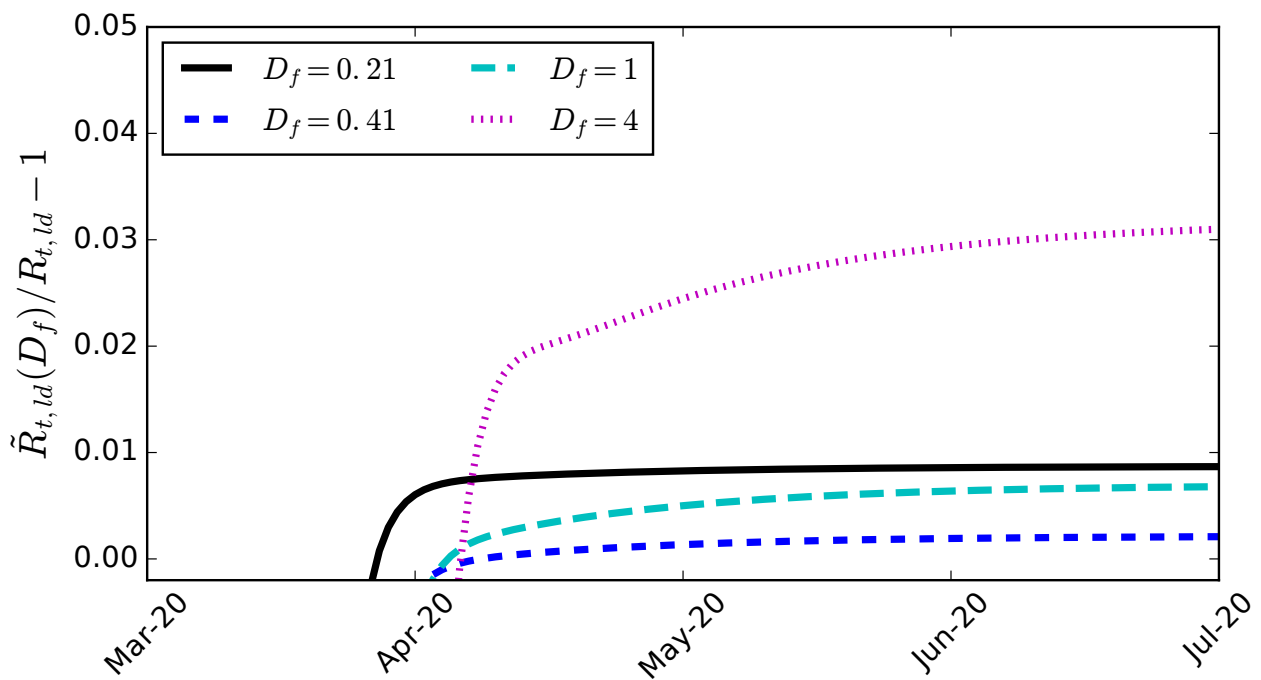
Figure 2. Relative difference between the effective reproduction number $\tilde{R}_{\text{t,ld}}$ for models with $N_f \simeq 0.14$, $R_{\text{t,ld}} \simeq 0.04$, corresponding to the 95% confidence upper limits on N_f, that would be inferred from the death rates assuming a counterfactual model with $N_f = 0$, compared with the maximum likelihood value for $R_{t,ld}$ for a model with $N_f = 0$. Shown for various values of D_f.

on $R_{t,\text{ld}}$ and the corresponding maximum likelihood values for N_f. The upper limits on N_f and $R_{t,\text{ld}}$ are not very sensitive to the fomite contamination duration D_f, and correspond to the pandemic's being spread almost entirely by either contaminated fomites or direct transmission, respectively. The overall maximum likelihood solution corresponds to $N_f = 0$ and $R_{t,\text{ld}} = 0.76$ for all values of $0.21 \le D_f \le 4$ d.

The power-series solutions in Sec. 2.2 show contaminated fomites affect the death rates in second order. The magnitude of the departure from the prediction for a constant reproduction number may be seen from the effective reproduction number that would be inferred from the death rates assuming a counterfactual model with no fomite contamination. Taking the exposure rate to be proportional to $\tilde{R}_{t,\text{ld}}(D_f) i s / D_i$, it follows from Eqs. (2.1) that $\tilde{R}_{t,\text{ld}}(D_f) = R_{t,\text{ld}} + (D_i/D_f)N_f f_*/i$. The effective reproduction numbers $\tilde{R}_{t,\text{ld}}$ are computed from the solutions to models corresponding to the 95% confidence upper limits on N_f and their corresponding maximum likelihood values $R_{t,\text{ld}}$ in Table 2 for the various values of fomite contamination duration D_f. Fig. 2 shows the fractional differences $\tilde{R}_{t,\text{ld}}(D_f)/R_{t,\text{ld}} - 1$, where $R_{t,\text{ld}}$ is the maximum likelihood value for the reproduction number for a model with $N_f = 0$. The effective reproduction numbers become time-dependent, increasing with time by an amount that depends on D_f. The fractional differences, however, are very small, exceeding 1% only when D_f is comparable to D_i. The effect of contaminated fomites is too small to be discernable from the population statistics without additional information.

The expectation value for the number of excess deaths from contaminated fomites is computed from the difference in the number of deaths predicted by a model with given values of $R_{t,\text{ld}}$ and $T_f > 0$ and the corresponding model with the same value of $R_{t,\text{ld}}$ and $T_f = 0$, averaged over all the models, weighting each by its likelihood. The expected number of excess deaths over the lockdown period ranges from about 13000–16000 (with fewer excess deaths for large D_f), corresponding to a fraction 60–70% of all deaths in this period. The probability distribution of the number of excess deaths, however, is very broad, as shown in the bottom panel of Fig. 1. No strong statement on the number of excess deaths resulting from contaminated fomite transmission may be made: any number from zero up to all cannot be excluded at the 95% confidence level.

3.2. CoMix study prior

The CoMix study in the UK provides additional information on the reduction in the number of social contacts per person during lockdown that limits the allowed range in the reproduction number in lockdown, breaking the degeneracy (co-linearity) between R_t and N_f in the effective reproduction number $\tilde{R}_t(N_f, D_f)$. For fomites with their transmittivity unchanged under lockdown conditions, the CoMix result on the reduction in the number of social contacts after lockdown is used to estimate a prior probability distribution for the reproduction number in lockdown, $R_{r,\text{ld}}$, as follows. The basic reproduction number found before lockdown is re-interpreted as an effective basic reproduction number $\tilde{R}_0 = R_0 + (D_i/D_f)N_f f_*/i$. For any given values of N_f and D_f, the value of $\tilde{R}_0$ at the moment of lockdown, at time t_{ld}, is used to provide an estimate for the actual basic reproduction number in the model, $R_0(N_f, D_f) = \tilde{R}_0 - (D_i/D_f)N_f f_*(t_{\text{ld}})/i(t_{\text{ld}})$. Under the assumption that the reproduction numbers are directly proportional to the number of social contacts, for any given reproduction number $R_{t,\text{ld}}$ during lockdown, a posterior probability density function for the model is constructed by multiplying the likelihood for the model, Eq. (2.9), by the probability density for the ratio $f_{\text{ld}} = R_{t,\text{ld}}/R_0(N_f, D_f)$, taken to be proportional to a normal distribution with mean $\bar{f}_{\text{ld}} = 0.26$ and standard deviation $\sigma_{f_{\text{ld}}} = 0.086$, as inferred from Jarvis et al. [24]. (It is noted in practice it is sufficient to use the small D_f limit
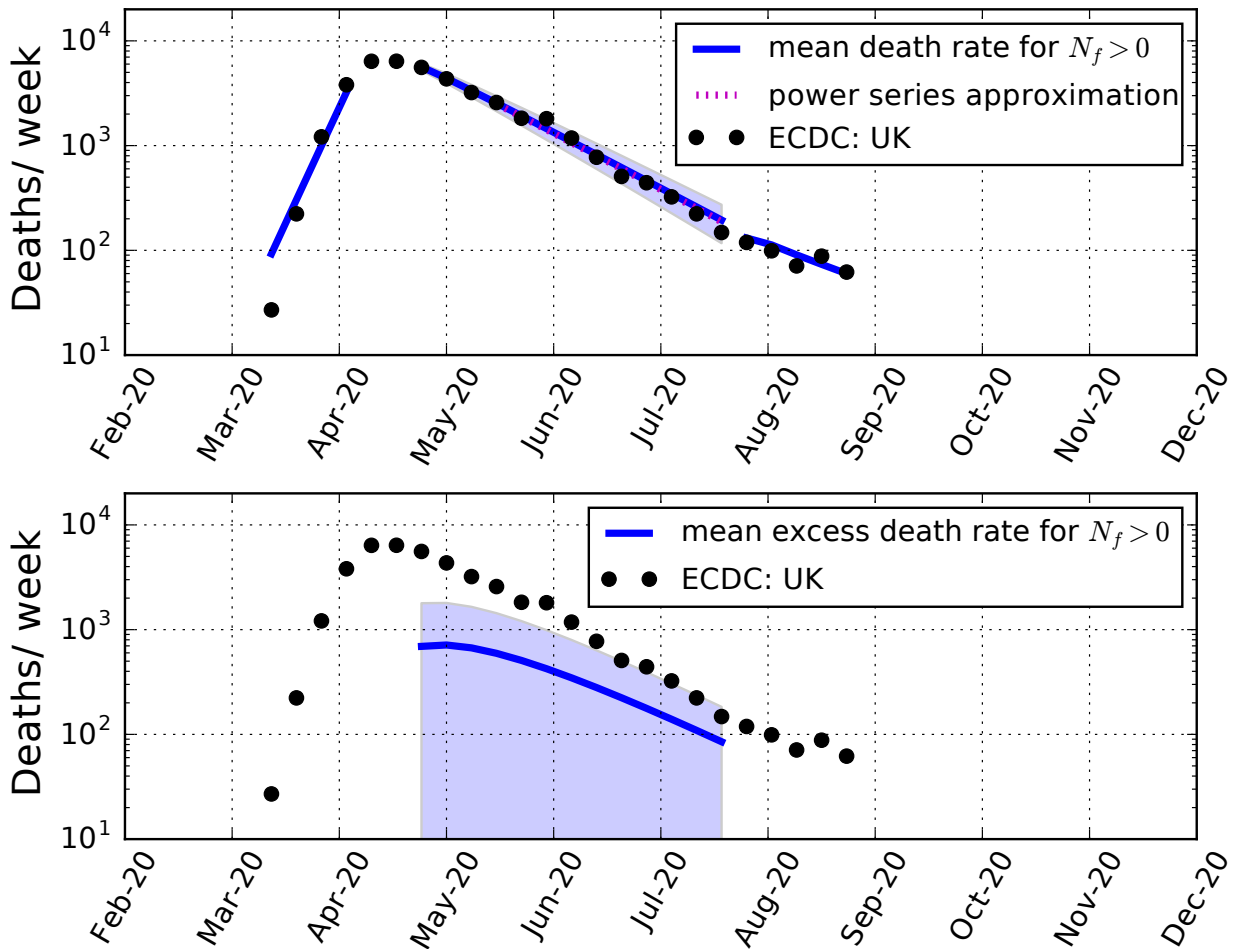
Figure 3. *Upper panel:* Weekly death rates in the UK. Black data points: the rates reported by the ECDC. Solid blue lines: Mean weekly deaths predicted for $D_f = 0.41$ d and assuming a uniform prior for N_f and a prior for $R_{t,ld}$ after lockdown based on the CoMix study. Also shown is the 95% range of uncertainty in the mean predicted number of deaths during lockdown (shaded region). Red dotted line: Power series approximate solution during the lockdown period (see Appendix). *Bottom panel:* Blue solid line: Mean predicted excess deaths per week arising from contaminated fomites, along with the 95% upper limit (shaded region).

D_f	N_f (95% CL)	$R_{\text{t,ld}}$ (M-L)	$R_{\text{t,ld}}$ (95% CL)	N_f (M-L)
d	d^{-1}			d^{-1}
0.21	0.034	0.59	0.77	0
0.41	0.035	0.59	0.77	0
1	0.034	0.58	0.77	0
4	0.028	0.61	0.77	0

Table 3. Model results for a uniform prior for N_f and a prior for $R_{\text{t,ld}}$ based on the CoMix study. The columns are: (1) fomite contamination duration (days); (2) 95% upper limit on N_f (per infectious person per day) and (3) the corresponding maximum posterior probability value for $R_{\text{t,ld}}$; (4) 95% upper limit on $R_{\text{t,ld}}$ and (5) the corresponding maximum posterior probability value for N_f (per infectious person per day).

for obtaining $R_0(N_f) = \tilde{R}_0 - D_i N_f$, as the difference in estimators is small compared with R_0.)

The marginal posterior probability distribution for $R_{\text{t,ld}}$, marginalised over N_f (as in Sec. 3.1, applied to the posterior probability density function defined here), is shown in Fig. 1 for $D_f = 0.41$ d. The results are nearly independent of D_f over $0.21 \leq D_f \leq 4$ d. In contrast to models with a uniform prior on $R_{\text{t,ld}}$, using the CoMix prior study corresponds to a maximum marginal posterior probability value for the reproduction number during lockdown of $R_{\text{t,ld}} = 0.74^{+0.05}_{-0.16}$ (95% CI), after marginalising over N_f. This may be compared with the most probable value for a model with $N_f = 0$ of $R_{\text{t,ld}} = 0.76^{+0.04}_{-0.03}$ (95% CI), so that allowing for contaminated fomites little affects the value but broadens the confidence interval.

By contrast, the marginal posterior probability distribution for N_f continues to be flat, peaking at $N_f = 0$. The marginalised 95% upper limit on N_f is $N_f \lesssim 0.035\,\text{d}^{-1}$ infectious person^{-1} for $0.21 \leq D_f \leq 1$ d and $N_f < 0.028\,\text{d}^{-1}$ infectious person^{-1} for $D_f = 4$ d, as shown in Table 3. Corresponding to these upper limits on N_f, the maximum posterior probability value for the reproduction number during lockdown is $R_{\text{t,ld}} = 0.6$. Marginalised over N_f, $R_{\text{t,ld}} < 0.77$ at 95% confidence. The corresponding maximum posterior probability values for N_f vanish for all values of D_f. The overall peak posterior probability density corresponds to $N_f = 0$ and $R_{\text{t,ld}} = 0.76$ for all values of $0.21 \leq D_f, \leq 4$ d. Consequently, conservatively no contaminated fomite signal is detected: the uncertainty in the reduction in the number of social contacts from the CoMix study is consistent with all of the reduction in the transmission being attributed to the reduction in direct contacts. The uncertainty in the reduction in the number of social contacts, however, is sufficiently small that a much more restrictive upper limit on the transmission rate by contaminated fomites may be placed compared with the case of a uniform prior on $R_{\text{t,ld}}$.

The mean weekly death rate for $D_f = 0.41$ d is shown in the upper panel of Fig. 3, along with the 95% confidence interval. The lower panel shows the mean excess numbers of weekly deaths for $N_f > 0$ compared with a counterfactual model having $N_f = 0$ (computed as described in Sec. 3.1), along with the 95% upper limit. Summing over the shown lockdown period gives an expectation value of about

4960 excess deaths, compared with about 22900 total deaths. This corresponds to an expectation value for the death excess from fomites of 22% of the total deaths from COVID-19. The probability density for the total number of excess deaths over the lockdown period is broad, but peaks at a lower number of excess deaths compared with the case of a uniform prior on $R_{\mathrm{t,ld}}$, as shown in the lower panel of Fig. 1. The 95% upper limit on the number of excess deaths is 12000, corresponding to 52% of all deaths. This is typified by a model for $D_f = 0.41$ d with $N_f = 0.035\,\mathrm{d}^{-1}$ infectious person^{-1} and $R_{\mathrm{t,ld}} = 0.59$ (see Table 3), for which 51% of the deaths during lockdown arise from contaminated fomites. Similar results are found for $D_f = 0.21$ and 1 d. The number of excess deaths for $D_f = 4$ d, however, is somewhat smaller. The expected number of excess deaths is about 4200 over the lockdown period, or 18% of all deaths during this time, with an upper limit of 10300 excess deaths (95% CL), or 45% of all deaths during lockdown.

4. Discussion

4.1. Parameter constraints

The use of compartmentalized population statistics in a SEIR model, extended to include contaminated fomites, is investigated as a possible means of constraining the contaminated fomite transmission rate N_f from the time dependence of the populations after a lockdown. The analysis is limited to fomites for which the transmittivity T_f remains unchanged by the lockdown. Without knowledge of the change in the reproduction number after lockdown is imposed, it is shown that it is not practically possible to separate the role of the fomites from the changing reproduction number using population statistics alone. Applied to the case of COVID-19 in the UK, adding a contaminated fomite contribution was not found to improve the agreement between the time dependence of the mortality rates following lockdown predicted by the extended SEIR model and the reported mortality rates, assuming uniform priors on N_f and reproduction number during lockdown $R_{\mathrm{t,ld}}$. The upper limits obtained are $N_f < (0.13 - 0.14)\,\mathrm{d}^{-1}$ infectious person^{-1} (decreasing with D_f) and $R_{\mathrm{t,ld}} < 0.72 - 73$ (increasing with D_f) (95% CL). The joint likelihood function for both N_f and $R_{\mathrm{t,ld}}$ has a sharp ridge at $R_{\mathrm{t,ld}} + D_i N_f \approx 0.76$, expressing their near statistical co-linearity. Whilst the formal maximum likelihood model corresponds to $N_f = 0$, the probability distribution for the number of excess deaths is broad. The expected number of excess deaths arising from contaminated fomites is 60–70% of the total deaths from COVID-19 during lockdown (decreasing with D_f), and the possibility that all deaths arose from contaminated fomites may not be excluded at better than 95–98% confidence (increasing with D_f).

Including the UK CoMix study results on the reduction in social contacts following the near complete lockdown imposed in March 2020 modifies the prior distribution on the reproduction number, allowing a tighter constraint to be placed on the transmission rate by contaminated fomites of $N_f \lesssim 0.03\,\mathrm{d}^{-1}$ infectious person^{-1} (95% CL) for $0.21 < D_f < 4$ d. The marginal posterior estimate of the reproduction number during lockdown is found to be $R_{\mathrm{t,ld}} = 0.74^{+0.05}_{-0.16}$ (95% CI), after marginalising over N_f. The marginal posterior probability distribution for $R_{\mathrm{t,ld}}$ is little sensitive to the addition of contaminated fomites, so that models without fomites should provide reliable estimates for the reproduction number even if contaminated fomites contribute to the overall transmission rate. The value for $R_{\mathrm{t,ld}}$ found here is consistent with other estimates, but on the lower end of the range [13].

To give the limits on N_f some context, the mean number C_f of potentially contaminatable objects a person may come into contact with per day must be specified. An estimate for the post is $C_f \simeq$

0.57 d^{-1} person^{-1} [34]. For food items, the Office for National Statistics estimates an average spend of £63.80 per week for an average household [39] of 2.4 members [40]. For an average product value of £2, this corresponds to $C_f \sim 2.5$ d^{-1} person^{-1} for post and food items combined. The upper limit allowing for the CoMix prior then corresponds to a contaminated fomite transmittivity upper limit of $T_f < 0.014$ (95% CL), or at most about 1 in 70 objects that comes into contact with an infectious person transmits the infection to a susceptible person.

The upper limit on T_f may be compared with QMRA estimates for the infection risk from fomites using stochastic-mechanistic modelling. Wilson et al. [55] find an infection risk from contact with a single contaminated fomite and subsequent self-inoculation event of ~ 0.03 for a contamination bio-burden of 10^4 genome copies per cm^2 (gc/cm^2) if 1% are infective, and an infection risk as high as 0.3 if 10% are infective. This is at the high end of the bio-burden range considered. For a bio-burden below 1 gc/cm^2, the infection risk is considerably smaller, less than 10^{-4}. Allowing for disinfection further reduces the risks.

Pitol et al. [44] find a somewhat smaller infection risk range of $10^{-4} - 10^{-2}$ (5th and 95th percentiles) for a bio-burden of 10^4 gc/cm^2. Measurements of bio-burdens in public spaces are considerably smaller. Even allowing for inefficiency in the recovery of samples, the bio-burdens obtained are below 1000 gc/cm^2 [1, 20]. Allowing for the prevalence of the infection, Pitol et al. [44] find for the range of bio-burdens considered a median (IQR) risk for a single touch of a fomite followed by self-inoculation through facial contact of 1.6×10^{-4} (2.0×10^{-5}, 1.4×10^{-3}) for the highest risk scenario considered of 5% prevalence and a high frequency of surface touching. This may be compared with the ratio of number of infections from touching a fomite per day to the number of fomites touched per day in the model presented here: $T_f f / (D_f C_f) = (T_f / D_f) f_* \simeq T_f i$, using the approximate relation $f_* \simeq D_f i$ (see Sec. 2.1). For an infectious fraction of the population of 5% ($i = 0.05$), this corresponds to an upper limit 7×10^{-4} (95% CL), similar to the infection risk found by Pitol et al. [44]. Their lowest risk scenario gives an infection risk smaller by several orders of magnitude. The upper limit found here is thus comparable to high risk scenario QMRA estimates using stochastic-mechanistic models.

Quantifying the impact of contaminated fomites in terms of the excess deaths compared with a counterfactual non-fomite model, when using the CoMix study informed prior on the reproduction number, the expected number of excess deaths during lockdown is found to be 22% of all COVID-19 deaths during this period. The 95% upper limit on the number of excess deaths is 52% of all deaths during lockdown for $0.2 \leq D_f \leq 1$ d. For a fomite contamination duration comparable to the infectious period, the limits are somewhat more restrictive. For $D_f = 4$ d, the expected number of excess deaths is 18% of all deaths during lockdown, with a 95% upper limit of 45%. Regardless of fomite contamination duration time, allowing for the CoMix study prior on the reproduction number during lockdown shows that it is highly unlikely that most deaths from COVID-19 were caused by transmission through lockdown-independent contaminated fomites.

It is emphasised that the probability distribution for the fraction of excess deaths is broad (Fig. 1): the results are consistent with no deaths ascribable to contaminated fomites. The expectation values found may be largely a result of the uncertainty in N_f, which arises from the uncertainty in the reduction factor of social contacts following lockdown. A more precise value for the reduction factor would narrow the probability distributions for N_f and for the number of excess deaths if N_f were actually smaller than the upper limit found here, resulting in a lower expectation value for the number of excess deaths from contaminated fomites.

4.2. Limitations of study

Placing constraints on the contribution of contaminated fomites to the spread of COVID-19 during lockdown requires some key assumptions. In this context, fomites may be divided into two types, those with a contact rate that depends on the number of social contacts and those independent of the number of social contacts. Only infections through the latter, such as by fomites that are part of essential services that continued through the lockdown like post deliveries and food purchases, may be constrained using the change in the time dependence of the population statistics following lockdown. Contaminated fomite transmission rates that scale with the number of social contacts likely scale with the reproduction number for direct transmission, and so their effects on the time dependence of the population statistics are indistinguishable from those of direct transmission. Some fomite contact rates, such as those in the workplace, may have decreased even faster than the decrease in the reproduction number following lockdown, as most workplaces were closed during the lockdown. No statement may be made about their role in the transmission of COVID-19 through a population analysis like the one presented here.

The strongest constraints on contaminated fomite transmission in this study rely on the measured change in the number of social contacts following lockdown from the CoMix study in the UK. It is assumed the change in the reproduction number is proportional to the change in the number of social contacts, and that the proportionality factor is independent of age. The measured reduction may be subject to several biases [24]: there is a possibility of recall bias, as the study requested information about the previous day; the sample may be subject to selection bias if preferably people observing the lockdown replied to the survey; also children were not interviewed, so that child-child contacts were inferred from the POLYMOD survey. The error range in the reduction in the number of social contacts limits the accuracy in the determination of the role of contaminated fomites in spreading the illness.

The models with contaminated fomites were found to result in a small increase in the transmission with time compared with the models without fomites. This difference accounts for the more stringent upper limits on the contribution by contaminated fomites with longer fomite contamination duration times. The increase may be interpreted as evidence for a slightly increasing reproduction number with time, in which case the contaminated fomite contribution would be even smaller. The alternative of a decreasing reproduction number with a larger contaminated fomite contribution than the upper limits found here cannot be ruled out, but it would seem unlikely the reproduction number would decrease in anticipation of an easing of the lockdown, and in any case this possibility would have only a small effect on the parameter limits found.

If the fomites considered were contaminated primarily by exhaled respiratory droplets or aerosols rather than by touch, the level of contamination may change with changing use of face-coverings. Face-coverings were not yet in common use before the Spring 2020 lockdown, so that in this case the upper limit on N_f found here may apply only after the lockdown.

5. Conclusions

Because of their persistence as a source of infection, contaminated fomites alter the time dependence of the compartmentalized populations of a SEIR model for an epidemic compared with direct transmission alone. The differences, however, are too small to detect when the duration of fomite contamination is shorter than the duration of the infectious phase. The use of uniform priors on the

reproduction number and contaminated fomite transmission factor does not permit very meaningful limits to be set on the contaminated fomite transmission rate based on the observed time dependence of the populations alone. By contrast, it is shown that by incorporating a measurement of the change in the number of social contacts when a lockdown is implemented, as provided by the CoMix study during the Spring 2020 COVID-19 lockdown in the UK, and under the assumption that the reproduction number scales with the number of social contacts, the model places a more restrictive upper limit on the role of contaminated fomites. The tightness of the upper limit depends on the accuracy with which the reduction in the number of social contacts has been measured.

Using data for the UK from the lockdown in March to July 2020 in conjunction with the reduction in social contacts from the CoMix study, it is found that contaminated fomites that act independently of a lockdown, such as delivered post or food packaging, contributed to fewer than about half (0.52, 95% CL) of the total deaths from COVID-19 during the lockdown, and most likely fewer than a quarter (0.22, 50% CL). Fewer than 1 in 70 (95% CL) contaminated fomites is found to transmit the infection. These limits are at the upper end of the range of estimates from QMRA analyses based on mechanistic models; most of the models obtain much smaller infection risks of COVID-19 from fomites in public spaces. While not directly applicable to the fomites considered here, the QMRA findings suggest much smaller transmission rates for post and food packaging than the upper limit found here. The QMRA estimates, however, are subject to the still unknown dose-response function for the SARS-CoV-2 virus. The SEIR analysis presented here follows a complementary approach by seeking instead to use the observed population dynamics to provide an upper limit on the degree to which some contaminated fomites transmitted COVID-19 within the UK. Although cruder in accuracy than full QMRA analyses, the method requires only the observed death rates, infected fatality fraction and reduction in numbers of social contacts under lockdown, along with a very weak dependence on fomite contamination durations, to obtain its constraints. The data for all of these were available by the end of the lockdown. Similar data in any future epidemic could allow an early estimate of the possible role of fomites, which could assist in informing public health policy regarding fomites while awaiting more complete QMRA analyses or epidemiological assessments.

6. Acknowledgments

Conflict of Interest: The author declares there is no conflict of interest.

A. Appendix

A.1. Existence and uniqueness of solutions

The existence and uniqueness of the solutions to Eqs. (2.1) is demonstrated using the following theorem [22]:

Theorem A.1 (Existence and Uniqueness). *Let the system of ordinary differential equations in real variables $y_i(t)$ for $i = 1$ to n for real t be*

$$\frac{d\mathbf{y}(t)}{dt} = \mathbf{f}(t, \mathbf{y}), \tag{A.1}$$

where $\mathbf{y} = (y_1, y_2, \ldots, y_n)$ *and* $\mathbf{f} = (f_1, f_2, \ldots, f_n)$ *for bounded, real single-valued functions* $f_i(t, \mathbf{y})$ *continuous in their $n + 1$ arguments defined on a real domain $\mathcal{D}$. Impose the Lipschitz condition*

$$|f_i(t, \mathbf{Y}) - f_i(t, \mathbf{y})| \leq \mathbf{K} \cdot |\mathbf{Y} - \mathbf{y}|, \tag{A.2}$$

for some n-dimensional real constant $\mathbf{K}$ (with each component non-negative), for $i = 1$ to n. Then there exists a unique and continuous solution $\mathbf{y}(t)$ to the system Eq. (A.1) for initial condition $\mathbf{y}(t_0) = \mathbf{y_0}$.

In preparation, the following lemma is first demonstrated:

Lemma A.1. *The solutions s, e, i, f_* to Eqs. (2.1) are non-negative and bounded from above for $t \geq t_0$ for initial conditions $s(t_0) \geq 0$, $e(t_0) \geq 0$, $i(t_0) \geq 0$, $f_*(t_0) \geq 0$.*

Proof: The solution for $s(t)$ is

$$s(t) = s(t_0) \exp\left[-\int_{t_0}^{t} dt' \left(\frac{R_t}{D_i} i(t') + \frac{N_f}{D_f} f_*(t')\right)\right] > 0. \tag{A.3}$$

Since initially $i(t) \geq 0$, the solution for $f_*(t)$ initially satisfies for $t > t_0$,

$$f_*(t) \geq f_*(t_0) \exp\left[-\frac{t - t_0}{D_i}\right] > 0. \tag{A.4}$$

It similarly follows that the solutions for $e(t)$ and $i(t)$ initially satisfy for $t > t_0$,

$$e(t) \geq e(t_0) \exp\left[-\frac{t - t_0}{D_e}\right] > 0 \tag{A.5}$$

and

$$i(t) \geq i(t_0) \exp\left[-\frac{t - t_0}{D_i}\right] > 0, \tag{A.6}$$

respectively. Subsequently e, i and f_* will maintain non-negative values as t continues to increase.

The recovered fraction r is governed by $dr/dt = i/D_i$. Since $i > 0$ for $t > t_0$, $r > 0$ for $t > t_0$. Adding dr/dt to the sum of Eqs. (2.1) gives, upon integration over t,

$$s(t) + e(t) + r(t) = s(t_0) + e(t_0) + r(t_0) + \int_{t_0}^{t} dt' \left[c_e(t') + c_i(t')\right], \tag{A.7}$$

expressing population conservation, allowing for an addition to the initial population through the introduction of exposed and infectious individuals at the respective (non-negative) rates c_e and c_i. It is assumed the additions to the initial population are finite, so that $c_e \to 0$ and $c_i \to 0$ as $t \to \infty$ and the time-integrals over c_e and c_i are convergent. Then all of s, e, i and r are bounded from above. The solution Eq. (2.4) shows that $f_*(t)$ is then also bounded from above.

The following theorem is now shown:

Theorem A.2. *The set of real solutions of Eqs. (2.1)*

$$\Sigma = \{(s, e, i, f_*) | s \geq 0, e \geq 0, i \geq 0, f_* \geq 0 \text{ for } t \geq t_0 \text{ and } s(t_0) \geq 0, e(t_0) \geq 0, i(t_0) \geq 0, f_*(t_0) \geq 0\} \quad \text{(A.8)}$$

exists and is unique.

Proof: Let $\mathbf{y} = (s, e, i, f_*)$ and express Eqs. (2.1) as

$$\frac{d\mathbf{y}}{dt} = \mathbf{f}(t, \mathbf{y}), \tag{A.9}$$

where $\mathbf{f} = (f_1, f_2, f_3, f_4)$ corresponds to the respective functions on the right hand side of Eqs. (2.1) for dy_j/dt for $j = 1$ to 4. Each function f_j is a product of linear factors of the variables $\mathbf{y}$, single-valued and continuous in t and $\mathbf{y}$. From Lemma A.1, all the functions $|f_j|$ are finite for all $t \geq t_0$. For each of $k = 1$ to 4, let K_k be an upper bound on $|\partial f_j/\partial y_k|$ over all $j = 1$ to 4. Then the Lipschitz condition Eq. (A.2) is satisfied. As an explicit example, consider $f_1 = -[(R_t/D_i)i + (N_f/D_f)f_*]s$. Then

$$
\begin{aligned}
|f_1(t, S, I, F_*) - f_1(t, s, i, f_*)| &= \left| \left(\frac{R_t}{D_i} I + \frac{N_f}{D_f} F_* \right) S - \left(\frac{R_t}{D_i} i + \frac{N_f}{D_f} f_* \right) s \right| \\
&= \left| \frac{R_t}{D_i} I(S - s) + \frac{R_t}{D_i}(I - i)s + \frac{N_f}{D_f} F_*(S - s) + \frac{N_f}{D_f}(F_* - f_*)s \right| \\
&= \left| \frac{\partial f_1(t, \mathbf{Y})}{\partial S}(S - s) + \frac{\partial f_1(t, \mathbf{y})}{\partial i}(I - i) + \frac{\partial f_1(t, \mathbf{y})}{\partial f_*}(F_* - f_*) \right| \\
&\leq \left| \frac{\partial f_1}{\partial s} \right|_{\max} |S - s| + \left| \frac{\partial f_1}{\partial i} \right|_{\max} |I - i| + \left| \frac{\partial f_1}{\partial f_*} \right|_{\max} |F_* - f_*|, \tag{A.10}
\end{aligned}
$$

the required Lipschitz condition. The cases for f_2, f_3 and f_4 follow through similarly. Therefore, all the conditions for Theorem A.1 apply. Lastly, from Lemma A.1 the solutions are non-negative for non-negative initial conditions. Consequently the set Σ exists and is unique.

A.2. Solution dynamics

Theorem A.3. *Let $(s, e, i, f_*) \in \Sigma$ (Eq. (A.8)). Suppose R_t, N_f and D_i are constant. Suppose both $c_e = 0$ and $c_i = 0$ by some time $t_c > t_0$. If $(R_t + N_f D_i)s(t_c) \leq 1$, then the infected fraction, given by $i + e + N_f f_*/(R_t + N_f D_i)$ and including contaminated fomites, decreases to zero as $t \to \infty$. If $(R_t + N_f D_i)s(t_c) > 1$, then the infected fraction first increases to a maximum value*

$$e(t_0) + i(t_0) + s(t_0) + \frac{N_r}{R_t + N_f D_i} f_*(t_0) - \frac{\log\left[(R_t + N_f D_i)s(t_0)\right]}{R_t + N_f D_i} - \frac{1}{R_t + N_f D_i} + \int_{t_0}^{t_c} dt' \, [c_e(t') + c_i(t')], \tag{A.11}$$

at $t = t_{\max}$, then decreases to zero as $t \to \infty$. The susceptible fraction $s(t)$ is a monotonically decreasing function and approaches a non-vanishing disease-free equilibrium value s_{eq} as $t \to \infty$ which is the unique root of Eq. (2.3). The equilibrium value is neutrally unstable for $(R_t + N_f D_i)s_{eq} > 1$ and stable otherwise.

Proof: The first two equations of Eqs. (2.1) may be combined into

$$\frac{d}{dt}\left(\log s - N_f f_*\right) = -(R_t + N_f D_i)\frac{i}{D_i}, \tag{A.12}$$

so that

$$-\frac{i}{D_i} = \frac{1}{R_t + N_f D_i} \frac{d}{dt}\left(\log s - N_f f_*\right). \tag{A.13}$$

Adding the second and third equations of Eqs. (2.1) and using Eq. (A.13) gives

$$\frac{d}{dt}(e+i) = -\frac{ds}{dt} + \frac{1}{R_t + N_f D_i} \frac{d}{dt}\left(\log s - N_f f_*\right) + c_e + c_i. \tag{A.14}$$

Integrating this over time gives the integral constraint on the solutions

$$\begin{aligned}
e(t) \quad + \quad & i(t) + s(t) + \frac{N_f f_*(t) - \log s(t)}{R_t + N_f D_i} \\
= \quad & e(t_0) + i(t_0) + s(t_0) + \frac{N_f f_*(t_0) - \log s(t_0)}{R_t + N_f D_i} + \int_{t_0}^{t} dt'\, [c_e(t') + c_i(t')], \tag{A.15}
\end{aligned}$$

valid for all $t \geq t_0$. For $t > t_c$ (so $c_e = c_i = 0$), dividing Eq. (A.14) by ds/dt gives

$$\frac{d}{ds}\left(e + i + \frac{N_f}{R_t + N_f D_i} f_*\right) = -1 + \frac{1}{s\left(R_t + N_f D_i\right)}. \tag{A.16}$$

From Eq. (A.3), $s(t)$ decreases monotonically with time. It follows then that for $s(t_c) \leq 1/(R_t + N_f D_i)$, $e + i + N_f f_*/(R_t + N_f D_i)$ decreases with time as $t \to \infty$. For $s(t_c) > 1/(R_t + N_f D_i)$, $e + i + N_f f_*/(R_t + N_f D_i)$ increases with time until $t = t_{\max}$ when $s(t_{\max}) = 1/(R_t + N_f D_f)$. From Eq. (A.15), the peak value $e + i + N_f f_*/(R_t + N_f D_i)$ attains is given by Eq. (A.11). As s continues to decrease for $t > t_{\max}$, $e + i + N_f f_*/(R_t + N_f D_i)$ will also decrease with time.

From Eq. (A.15), s must asymptotically approach a value $s_{\mathrm{eq}} > 0$, so that $ds/dt \to 0$ as $t \to \infty$. From Eqs. (2.1), it then follows that $i \to 0$ and $f_* \to 0$ as $t \to \infty$, and so also $df_*/dt \to 0$. It also follows from Eqs. (2.1) that $de/dt \to -e/D_e$, so that $e(t) \to C \exp(-t/D_e) \to 0$ for some constant C as $t \to \infty$. Then $de/dt \to 0$ and $di/dt \to 0$. So $s = s_{\mathrm{eq}}$ corresponds to a disease-free equilibrium given by the unique root of Eq. (2.3), from Eq. (A.15). It follows from Eq. (A.16), that if an infectious individual or contaminated fomite is introduced at this point, so that once again $ds/dt < 0$, then $e + i + N_f f_*/(R_t + N_f D_i)$ will increase with time if $s_{\mathrm{eq}} > 1/(R_t + N_f D_i)$ and decrease otherwise. Since $d[e + i + N_f f_*/(R_t + N_f D_i)]/dt = 0$ initially for $s_{\mathrm{eq}} = 1/(R_t + N_f D_i)$, the (in)stability is neutral.

If an exposed individual is introduced, then $ds/dt = 0$ still holds so that Eq. (A.16) no longer provides a stability criterion. The criterion, however, is unchanged, as may be demonstrated by expanding the solution for $e(t)$ near the equilibrium point. Suppose $s(t_0) = s_{\mathrm{eq}}$, $e(t_0) > 0$, $i(t_0) = 0$ and $f_*(t_0) = 0$. For small $t > t_0$, Eqs. (2.1) is solved to second order in $(t - t_0)$ by

$$\begin{aligned}
s(t) &\sim s_{\mathrm{eq}} - \frac{R_t}{D_i D_e} e_0 (t - t_0) - \frac{1}{2} \frac{R_t}{D_i D_e} e_0 s_{\mathrm{eq}} (t - t_0)^2, \\
e(t) &\sim e_0 - \frac{1}{D_e} e_0 (t - t_0) + \frac{1}{2} \frac{e_0}{D_i D_e} \left(R_t s_{\mathrm{eq}} + \frac{D_i}{D_e}\right)(t - t_0)^2, \\
i(t) &\sim \frac{e_0}{D_e}(t - t_0) - \frac{1}{2} \frac{e_0}{D_i D_e}\left(1 + \frac{D_i}{D_e}\right)(t - t_0)^2, \\
f_*(t) &\sim \frac{1}{2} \frac{e_0}{D_e}(t - t_0)^2, \tag{A.17}
\end{aligned}$$

as may be verified by direct substitution. Then

$$\frac{d}{dt}\left(e + i + \frac{N_f}{R_t + N_f D_i}f_*\right) \sim \frac{e_0}{D_i D_e}R_t\left(s_{\text{eq}} - \frac{1}{R_t + N_f D_i}\right)(t - t_0). \tag{A.18}$$

A.3. Power-series solutions

Power-series solutions of Eqs. (2.1) in r are constructed by first dividing the equations by $dr/dt = i/D_i$ to transform them to

$$\begin{aligned}
\frac{ds}{dr} &= -R_t s - \frac{D_i}{D_f}N_f \frac{s}{i}f_*, \\
\frac{de}{dr} &= R_t s + \frac{D_i}{D_f}N_f \frac{s}{i}f_* - \frac{D_i}{D_e}\frac{e}{i} + c_e \frac{D_i}{i}, \\
\frac{di}{dr} &= \frac{D_i}{D_e}\frac{e}{i} - 1 + c_i \frac{D_i}{i}, \\
\frac{df_*}{dr} &= D_i - \frac{D_i}{D_f}\frac{f_*}{i}.
\end{aligned} \tag{A.19}$$

Power-series solutions around $r = r_0 = r(t_0)$ after a time t_0 are assumed:

$$s(r) = s_0 + \sum_{n=1}^{\infty} s_n(r - r_0)^n, \qquad e(r) = e_0 + \sum_{n=1}^{\infty} e_n(r - r_0)^n, \qquad i(r) = i_0 + \sum_{n=1}^{\infty} i_n(r - r_0)^n. \tag{A.20}$$

It is numerically convenient to use the integrated solution for the contaminated fomite term:

$$\begin{aligned}
f_*(r) &= f_*(r_0)\exp\left[-\int_{r_0}^{r} dr' \frac{D_i}{D_f}\frac{1}{i(r')}\right] \\
&+ D_i \exp\left[-\int_{r_0}^{r} dr' \frac{D_i}{D_f}\frac{1}{i(r')}\right]\int_{r_0}^{r} dr'' \exp\left[\int_{r_0}^{r'} dr'' \frac{D_i}{D_f}\frac{1}{i(r'')}\right].
\end{aligned} \tag{A.21}$$

To second order, the coefficients are

$$s_1 = -\tilde{R}_{t0}s_0, \qquad s_2 = \frac{1}{2}\tilde{R}_{t0}^2 s_0 - \frac{1}{2}\frac{D_i}{D_f}N_f\left(1 - \frac{D_i}{D_e}\frac{e_0}{i_0} - \frac{D_i}{D_f}\right)\frac{f_*(r_0)s_0}{i_0^2} - \frac{1}{2}\frac{D_i^2}{D_f}N_f \frac{s_0}{i_0}, \tag{A.22}$$

$$e_1 = \tilde{R}_{t0} - \frac{D_i}{D_e}\frac{e_0}{i_0}, \tag{A.23}$$

$$\begin{aligned}
e_2 &= -\frac{1}{2}\tilde{R}_{t0}^2 s_0 - \frac{D_i}{2D_e i_0}\left\{\tilde{R}_{t0}s_0 + \frac{e_0}{i_0}\left[1 - \frac{D_i}{D_e}\left(1 + \frac{e_0}{i_0}\right)\right]\right\} \\
&+ \frac{1}{2}\frac{D_i}{D_f}N_f \frac{s_0}{i_0}\left\{D_i + \frac{f_*(r_0)}{i_0}\left[1 - \frac{D_i}{D_f}\left(1 + \frac{D_f}{D_e}\frac{e_0}{i_0}\right)\right]\right\},
\end{aligned} \tag{A.24}$$

and

$$i_1 = \frac{D_i}{D_e}\frac{e_0}{i_0} - 1, \qquad i_2 = \frac{D_i}{2D_e i_0}\left\{\tilde{R}_{t0}s_0 + \frac{e_0}{i_0}\left[1 - \frac{D_i}{D_e}\left(1 + \frac{e_0}{i_0}\right)\right]\right\}, \tag{A.25}$$

where the effective reproduction number $\tilde{R}_{t0} = R_t + (D_i/D_f)N_f f_*(r_0)/i_0$ has been defined.

The forms of the coefficients show that to first order, the contaminated fomite term does not affect the time dependence of the populations other than through a re-scaling of R_t to $\tilde{R}_{t0}$. At second order, the time dependence of the susceptible and exposed populations show additional contributions from the contaminated fomites (through $f_*(r_0)$) that are not eliminated by a re-scaling, whilst the time dependence of the infectious population, in contrast, may still be re-scaled to second order. Using the expression for i to second order, Eq. (A.21) becomes

$$\begin{aligned} f_*(r) &\simeq f_*(r_0)\left[\frac{y_+(r)}{y_+(r_0)}\frac{y_-(r_0)}{y_-(r)}\right]^\delta \\ &+ \frac{D_i}{4i_2\Delta(1+\delta)}y_+(r)y_-(r)\left\{\left[\frac{y_+(r)}{y_+(r_0)}\frac{y_-(r_0)}{y_-(r)}\right]^{1+\delta} - 1\right\}, \end{aligned} \tag{A.26}$$

where $y_\pm(r) = \Delta \pm [i_1 + 2i_2(r - r_0)]$, $\Delta = (i_1^2 - 4i_0 i_2)^{1/2}$ and $\delta = D_i/(D_f\Delta)$. (For applications here, $i_1^2 - 4i_0 i_2 > 0$.)

The time dependence of the populations may be expressed as a function of t through

$$t = t_0 + D_i \int_0^{r-r_0} \frac{dx}{i_0 + i_1 x + i_2 x^2} = \frac{D_i}{\Delta}\log\left[\frac{y_-(r)}{y_+(r)}\right]. \tag{A.27}$$

An example solution is illustrated in the upper panel of Fig. 3 for a solution at the 98% upper limit of $N_f = 0.042$ allowing for the CoMix prior, and the corresponding maximum likelihood value $R_{\text{t,ld}} = 0.55$. The predicted number of deaths agrees with the numerical solution for these parameter values to within 1%.

References

1. Abrahão, J., *et al.*, 2021. Detection of sars-cov-2 rna on public surfaces in a densely populated urban area of brazil: A potential tool for monitoring the circulation of infected patients. Sci Tot Environ. 766. doi:`10.1016/j.scitotenv.2020.142645`.

2. Al-Ansary, L., Bawazeer, G., Beller, E., *et al.*, 2020. Physical interventions to interrupt or reduce the spread of respiratory viruses. part 2 - hand hygiene and other hygiene measures: systematic review and meta-analysis doi:`10.1101/2020.04.14.20065250`.
   (Last accessed 14 June 2021).

3. Aldila, D., 2020. Cost-effectiveness and backward bifurcation analysis on covid-19 transmission model considering direct and indirect transmission. Commun. Math. Biol. Neurosci. 2020. doi:`10.28919/cmbn/4779`.

4. Ault, A., 2020. Mail handlers used to poke holes in envelopes to battle germs and viruses. Smiths Mag.
   (Last accessed 20 October 2021).

5. Azimi, P., Keshavarz, Z., Laurent, J., Stephens, B., Allen, J., 2021. Mechanistic transmission modeling of covid-19 on the diamond princess cruise ship demonstrates the importance of aerosol transmission. PNAS 118. doi:`10.1073/pnas.2015482118`.

6. Barker, J., Stevens, D., Bloomfield, S., 2001. Spread and prevention of some common viral infections in community facilities and domestic homes. J. Appl. Microbiol. 91, 7–21. doi:`10.1046/j.1365-2672.2001.01364.x`.

7. Belluco, S., Mancin, M., Marzoli, F., *et al.*, 2021. Prevalence of sars-cov-2 rna on inanimate surfaces: a systematic review and meta-analysis. Eur J Epidem doi:`10.1007/s10654-021-00784-y`.
(Last accessed 24 September 2021).

8. Boone, S., Gerba, C., 2007. Signifance of fomites in the spread of respiratory and enteric viral disease. Appl. Environ. Microbiol. 73, 1687–1696. doi:`10.1128/AEM.02051-06`.

9. Chang, A., Schnall, A., Law, R., *et al.*, 2020. Exposures and temporal associations with covid-19 - national poison data system, united states, january 1, 2020 - march 31, 2020. CDC MMWR Morb. Mortal Wkly Rep 69, 496–498. doi:`10.15585/mmwr.mm6916e1`.

10. Colaneri, M., Seminari, E., Novati, S., *et al.*, 2020. Severe acute respiratory syndrome coronavirus 2 rna contamination of inanimate surfaces and virus viability in a health care emergency unit. Clin Microbiol Infect. 26, 1094.e1–1094.e5. doi:`10.1016/j.cmi.2020.05.009`.

11. David, J., Iyaniwura, S., Ward, M., Brauer, F., 2020. A novel approach to modelling the spatial spread of airborne diseases: an epidemic model with indirect transmission. Math Biosci Eng 17, 3294–3328. doi:`10.3934/mbe.2020188`.

12. Davies, N., Kucharski, A., Eggo, R., Gimma, A., Edmunds, W., 2020. Effects of non-pharmaceutical interventions on covid-19 cases, deaths, and demand for hospital services in the uk: a modelling study. Lancet Public Health 5, e375–e385. doi:`10.1016/S2468-2667(20)30133-X`.

13. DHSC/SAGE, 2021. The r value and growth rate. Department of Health and Social Care (DHSC) and Scientific Advisory Group for Emergencies (SAGE). URL: `https://www.gov.uk/guidance/the-r-value-and-growth-rate`.
(Last accessed 15 June 2021).

14. du Plessis, L., McCrone, J., Zarebski, A., *et al.*, 2020. Establishment & lineage dynamics of the sars-cov-2 epidemic in the uk doi:`10.1101/2020.10.23.20218446`.
(Last accessed 14 June 2021).

15. Flaxman, S., Mishra, S., Gandy, H., *et al.*, 2020. Estimating the effects of non-pharmaceutical interventions on covid-19 in europe. Nature 584, 257–261. doi:`10.1038/s41586-020-2405-7`.

16. FSA, . Guidance for consumers on coronavirus (covid-19) and food. Food Standards Agency Guidance. URL: `https://www.gov.uk/government/publications/guidance-for-consumers-on-coronavirus-covid-19-and-food/guidance-for-consumers-on-coronavirus-covid-19-and-food`.
(Last accessed 25 October 2021).

17. Goldman, E., 2021. Sars wars: the fomites strike back. Appl Environ Microbiol. 87. doi:`10.1128/AEM.00653-21`.

18. Goldmann, D., 2000. Transmission of viral respiratory infections in the home. Pediatr Infect Dis J. 19, S97–102.

19. Harbourt, D., Haddow, A., Piper, A., *et al.*, 2020. Modeling the stability of severe acute respiratory syndrome coronavirus 2 (sars-cov-2) on skin, currency, and clothing. PLoS Negl Trop Dis 14, e0008831. doi:`10.1371/journal.pntd.0008831`.

20. Harvey, A., Fuhrmeister, E., Cantrell, M., Pitol, A., Swarthout, J., Powers, J., Nadimpalli, M., Julian, T., Pickering, A., 2021. Longitudinal monitoring of sars-cov-2 rna on high-touch surfaces in a community setting. Environ. Sci. Technol. Lett. 8, 168–175. doi:`10.1021/acs.estlett.0c00875`.

21. Hethcote, H., 2009. The basic epidemiology models: models, expressions for r_0, parameter estimation, and applications, in: Ma, S., Xia, Y. (Eds.), Mathematical Understanding Of Infectious Disease Dynamics. World Scientific Publishing Co. Pte. Ltd, Singapore. volume 16 of *Lecture Notes Series, Institute For Mathematical Sciences, National University Of Singapore*. chapter 1, pp. 1–62.

22. Ince, E., 1956 - 1926. Ordinary differential equations. Dover Publications, New York.

23. Iyaniwura, S., Rabiu, M., David, J., Kong, J., 2021. Assessing the impact of adherence to non-pharmaceutical interventions and indirect transmission on the dynamics of covid-19: a mathematical modelling study. Math Biosci Eng 18, 8905–8932. doi:`10.3934/mbe.2021439`.

24. Jarvis, C., Van Zandvoort, K., Gimma, A., *et al.*, 2020. Quantifying the impact of physical distance measures on the transmission of covid-19 in the uk. BMC Med 18. doi:`10.1186/s12916-020-01597-8`.

25. Ji, W., Li, X., Chen, S., Ren, L., 2021. Transmission of sars-cov-2 via fomite, especially cold chain, should not be ignored. Proc Natl Acad Sci USA 118.

26. Jiang, F., Jiang, X.L., Wang, Z.G., Meng, Z.H., Shao, S.F., Anderson, B., Ma, M.J., 2020. Detection of severe acute respiratory syndrome coronavirus 2 rna on surfaces in quarantine rooms. Emerg Infect Dis. 26, 2162–2164. doi:`10.3201/eid2609.201435`.

27. Kraay, A., Hayashi, M., Hernandez-Ceron, N., Spicknall, I., Eisenberg, M., Meza, R., Eisenberg, J., 2018. Fomite-mediated transmission as a sufficient pathway: a comparative analysis across three viral pathogens. BMC Infect Dis. 18. doi:`10.1186/s12879-018-3425-x`.

28. Kutter, J., Spronken, M., Fraaij, P., Fouchier, R., Herfst, S., 2018. Transmission routes of respiratory viruses among humans. Curr Opin Virol. 28, 142–151. doi:`10.1016/j.coviro.2018.01.001`.

29. Leung, N., 2021. Transmissibility and transmission of respiratory viruses. Nature Revs Microbiol. doi:`10.1038/s41579-021-00535-6`.

30. Lewis, D., 2021. Covid-19 rarely spreads through surfaces. so why are we still deep cleaning? Nature 590, 26–28. doi:`10.1038/d41586-021-00251-4`.

31. Lio, C., Cheon, H., Lei, C., *et al.*, 2021. Effectiveness of personal protective health behaviour against covid-19. BMC Public Health 21, 827. doi:`10.1186/s12889-021-10680-5`.

32. Liu, P., Yang, M., Zhao, X., Guo, Y., Wang, L., Zhang, J., *et al.*, 2020. Cold-chain transportation in the frozen food industry may have caused a recurrence of covid-19 cases in destination: Successful

isolation of sars-cov-2 virus from the imported frozen cod package surface. Biosaf Health. 2, 199–201.

33. Mayoclin., 2021. Mayoclinic. URL: `https://www.mayoclinic.org/diseases-conditions/coronavirus/expert-answers/can-coronavirus-spread-food-water/faq-20485479`.
(Last accessed 20 October 2021).

34. Meiksin, A., 2020. Dynamics of covid-19 transmission including indirect transmission mechanisms: a mathematical analysis. Epidemiology and Infection 148, 1–7. doi:`10.1017/S0950268820002563`.

35. Morawska, L., Milton, D., 2020. It is time to address airborne transmission of coronavirus disease 2019 (covid-19). Clin Infect Dis. 71, 2311–2313. doi:`10.1093/cid/ciaa939`.

36. NCIRD, 2021. Sars-cov-2 and surface (fomite) transmission for indoor community environments. CDC COVID-19 Science Briefs. National Center for Immunization and Respiratory Diseases, (NCIRD). URL: `https://www.ncbi.nlm.nih.gov/books/NBK570437/#!po=1.11111`.
(Last accessed 25 October 2021).

37. Onakpoya, I., Heneghan, C., Spencer, E., *et al.*, 2021. Sars-cov-2 and the role of fomite transmission: a systematic review [version3; peer review: 2 approved]. F1000Research 10. doi:`10.12688/f1000research.51590.3`.

38. Ong, S., Tan, Y., Chia, P., *et al.*, 2020. Air, surface environmental, and personal protective equipment contamination by severe acute respiratory syndrome coronavirus 2 (sars-cov-2) from a symptomatic patient. JAMA 323, 1610–1612. doi:`10.1001/jama.2020.3227`.

39. ONS, 2020. Expenditure on food and non-alcoholic drinks by place of purchase: table a2. Office for National Statistics (ONS). URL: `https://www.ons.gov.uk`.
(Last accessed 11 June 2021).

40. ONS, 2021. Families and households in the uk: 2020. Statistical bulletin. Office for National Statistics (ONS). URL: `https://www.ons.gov.uk`.
(Last accessed 11 June 2021).

41. Otter, J., Donskey, C., Yezli, S., Douthwaite, S., Goldenberg, S., Weber, D., 2016. Air, surface environmental, and personal protective equipment contamination by severe acute respiratory syndrome coronavirus 2 (sars-cov-2) from a symptomatic patient. J Hosp Infec. 92, 235–250. doi:`10.1016/j.jhin.2015.08.027`.

42. Pastorino, B., Touret, F., Gilles, M., de Lamballerie, X., Charrel, R., 2020. Prolonged infectivity of sars-cov-2 in fomites. Emerg Infect Dis. 26, 2256–2257. doi:`10.3201/eid2609.201788`.

43. PHAS, 2020. The infection fatality rate of COVID-19 in Stockholm. Technical Report. Folkhälsomyndigheten: Public Health Agency of Sweden (PHAS). URL: `https://www.folkhalsomyndigheten.se/publicerat-material/`.
(Last accessed 28 May 2021).

44. Pitol, A., Julian, T., 2021. Community transmission of sars-cov-2 by surfaces: risks and risk reduction strategies. Environ. Sci. Technol. Lett. 8, 263–269. doi:`10.1021/acs.estlett.0c00966`.

725   45. Rushton, S., Sanderson, R., Reid, W., Shirley, M., Harris, J., Hunter, P., O'Brien, S., 2019. Transmission routes of rare seasonal diseases: the case of norovirus infections. Phil Trans R Soc. B 374. doi:`10.1098/rstb.2018.0267`.

46. Russell, T., Hellewell, J., Jarvis, C., *et al.*, 2020. Estimating the infection and case fatality ratio for coronavirus diseases (covid-19) using age-adjusted data from the outbreak on the diamond
730   princess cruised ship, february 2020. Euro Serveillance 25. doi:`10.2807/1560-7917.ES.2020.25.12.2000256`.

47. Sobolik, J., Sajewski, E., Jaykus, L.A., Cooper, D., Lopman, B., Kraay, A., Ryan, P., *et al.*, 2021. Low risk of sars-cov-2 transmission via fomite, even in cold-chain doi:`10.1101/2021.08.23.21262477`.
735   (Last accessed 27 October 2021).

48. Stephens, B., Azimi, P., Thoemmes, M., Heidarinejad, M., Allen, J., Gilbert, J., 2019. Microbial exchange via fomites and implications for human health. Curr Poll Reps. 5, 198–213. doi:`10.1007/s40726-019-00123-6`.

49. Sze-To, G., Yang, Y., Kwan, J., Yu, S., Chao, C., 2014. Effects of surface material, ventilation,
740   and human behavior on indirect contact transmission risk of respiratory infection. Risk Analys. 34, 818–830. doi:`10.1111/risa.12144`.

50. UNICEF, . Cleaning and hygiene tips to help keep the covid-19 virus out of your home. URL: `https://www.unicef.org/romania/stories/cleaning-and-hygiene-tips-help-keep-covid-19-virus-out-your-home`.
745   (Last accessed 25 October 2021).

51. van Doremalen, N., Bushmaker, T., Morris, D., *et al.*, 2020. Aerosol and surface stability of sars-cov-2 as compared with sars-cov-1. N Engl J Med 382, 1564–1567. doi:`10.1056/NEJMc2004973`.

52. WHO, 2016. Quantitative microbial risk assessment. application for water safety management.
750   Scientific Brief. World Health Organization (WHO). URL: `https://apps.who.int/iris/handle/10665/246195`.
(Last accessed 14 November 2021).

53. WHO, 2020. Transmission of sars-cov-2: implications for infection prevention precautions. Scientific Brief. World Health Organization (WHO).
755   URL: `https://www.who.int/news-room/commentaries/detail\/transmission-of-sars-cov-2-implications-for-infection-\prevention-precautions`.
(Last accessed 25 May 2021).

54. Wijaya, K., Ganegoda, N., Jayathunga, Y., Götz, T., Schäfer, M., Heidrich, P., 2021. An epidemic
760   model integrating direct and fomite transmission as well as household structure applied to covid-19. J Math Indus. 11. doi:`10.1186/s13362-020-00097-x`.

55. Wilson, A., Weir, M., Bloomfield, S., Scott, E., Reynolds, K., 2021. Modeling covid-19 infection risks for a single hand-to-fomite scenario and potential risk reductions offered by surface disinfection. Am J Infec Contr. 49, 846–848. doi:`10.1016/j.ajic.2020.11.013`.

56. Zhong, H., Wang, W., 2020. Mathematical analysis for covid-19 resurgence in the contaminated environment. Math Biosci Eng. 17, 6909–6927. doi:`10.3934/mbe.2020357`.

57. Zuo, Y., Uspal, W., Wei, T., 2020. Airborne transmission of covid-19: Aerosol dispersion, lung deposition, and virus-receptor interactions. ACS Nano 14, 16502–16524. doi:`10.1021/acsnano.0c08484`.

AIMS Press